Plant Biotechnology Journal
Open Access

Plant Biotechnology Journal (2022) **20**, pp. 920–933 doi: 10.1111/pbi.13773

A single nucleotide deletion in the third exon of *FT-D1* increases the spikelet number and delays heading date in wheat (*Triticum aestivum* L.)

Zhaoyan Chen[1,2,†], Wensheng Ke[1,2,†], Fei He[1,2], Lingling Chai[1,2], Xuejiao Cheng[3], Huanwen Xu[1,2], Xiaobo Wang[1,2], Dejie Du[1,2], Yidi Zhao[1,2], Xiyong Chen[4], Jiewen Xing[1,2], Mingming Xin[1,2], Weilong Guo[1,2], Zhaorong Hu[1,2], Zhenqi Su[1,2], Jie Liu[1,2], Huiru Peng[1,2], Yingyin Yao[1,2], Qixin Sun[1,2] and Zhongfu Ni[1,2,*]

[1]*State Key Laboratory for Agrobiotechnology, Key Laboratory of Crop Heterosis and Utilization (MOE), Key Laboratory of Crop Genetic Improvement, China Agricultural University, Beijing, China*

[2]*National Plant Gene Research Centre, Beijing, China*

[3]*State Key Laboratory for Crop Genetics and Germplasm Enhancement, JCIC-MCP, CIC-MCP, Nanjing Agricultural University, Nanjing, China*

[4]*Hebei Crop Genetic Breeding Laboratory, Institute of Cereal and Oil Crops, Hebei Academy of Agriculture and Forestry Sciences, Shijiazhuang, China*

Received 29 July 2021;
revised 2 December 2021;
accepted 24 December 2021.
**Correspondence* (Tel 86-010-62734421; email nizf@cau.edu.cn)
†These authors contributed equally to this work.

Keywords: Wheat (*Triticum aestivum* L.), spikelet number, heading date, *FT-D1*, STARP, CRISPR/Cas9.

Summary

The spikelet number and heading date are two crucial and correlated traits for yield in wheat. Here, a quantitative trait locus (QTL) analysis was conducted in F_8 recombinant inbred lines (RILs) derived from crossing two common wheats with different spikelet numbers. A total of 15 stable QTL influencing total spikelet number (TSN) and heading date (HD) were detected. Notably, *FT-D1*, a well-known flowering time gene in wheat, was located within the finely mapped interval of a major QTL on 7DS (*QTsn/Hd.cau-7D*). A causal indel of one G in the third exon of *FT-D1* was significantly associated with total spikelet number and heading date. Consistently, CRISPR/Cas9 mutant lines with homozygous mutations in *FT-D1* displayed an increase in total spikelet number and heading date when compared with wild type. Moreover, one simple and robust marker developed according to the polymorphic site of *FT-D1* revealed that this one G indel had been preferentially selected to adapt to different environments. Collectively, these data provide further insights into the genetic basis of spikelet number and heading date, and the diagnostic marker of *FT-D1* will be useful for marker-assisted pyramiding in wheat breeding.

Introduction

Wheat is one of the largest grain crops in the world today. Continuing population growth is increasing the demand for the development of novel ways to enhance its yield potential (Boden *et al*., 2015). Wheat yield can be divided into three components, including thousand grain weight (TGW), grain number per spike (GNS) and spike number per hectare (Simmonds *et al*., 2014). Generally, GNS can be broken down into the spikelet number and grains per spikelet (Quarrie *et al*., 2006). An increased number of fertile florets per spikelet could probably increase in yield potential in wheat (Sakuma *et al*., 2019; Sakuma and Schnurbusch, 2020). Thereby, modifying the spikelet number could be a strategy to improve yield potential in wheat, since it is associated with a higher GNS (Lewis *et al*., 2008).

Spikelet number is quantitative in nature and controlled by numbers of genes/QTL (quantitative trait loci). Identification of DNA markers associated with spikelet number would allow marker-assisted selection (MAS) and increase the efficiency for improving yield potential during breeding. Over the past two decades, the successful application of quantitative-genetic methodology facilitated the identification of QTL for spikelet number (Cui *et al*., 2012). Many QTL across multiple genetic backgrounds have been identified on almost all 21 chromosomes in wheat (Chen *et al*., 2020b; Deng *et al*., 2011; Ma *et al*., 2007, 2019; Yao *et al*., 2019; Zhai *et al*., 2016; Zhang *et al*., 2015; Zhou *et al*., 2017). Only few genes involved in spikelet number have been characterized through map- or homology-based cloning, such as *TaMOC1*, *TaAPO1*, *TB1* and *WFZP* (Dixon *et al*., 2018b; Du *et al*., 2021; Muqaddasi *et al*., 2019; Zhang *et al*., 2015). Despite these efforts, cloning of the QTL controlling spikelet number will provide an important entry for studying the gene network involved in the spike development in wheat (Lewis *et al*., 2008).

Heading date is usually determined by vernalization requirement, photoperiodic response and earliness *per se*, which is crucial for wide adaptation to diverse environments and affecting crop yield (Gawroński *et al*., 2014; Lewis *et al*., 2008; Shimada *et al*., 2009; Yasuda and Shimoyama, 1965; Zhang *et al*., 2018). Vernalization is defined as the acquisition of the ability to flower by a low-temperature treatment (Chouard, 1960; Fu *et al*., 2005). Genetic studies demonstrated that vernalization process is controlled by at least four critical genes designated *Vrn-1*, *Vrn-2*, *Vrn-3* and *Vrn-4* (Kippes *et al*., 2015; Yan *et al*., 2003, 2004, 2006). Allelic variations in *Ppd-1* influence sensitivity to daylength in temperate cereals (Boden *et al*., 2015; Gauley and Boden, 2021). Wheat varieties that are photoperiod sensitive required a period of long days to permit initiation of the floral primordia without undue delay (Worland, 1996). Earliness *per se* is described as the variation in flowering observed once photoperiod and vernalization requirements were fully satisfied (Gomez *et al*., 2014). The previous studies have shown a positive correlation between

spikelet number and heading date (Boden *et al*., 2015; Lewis *et al*., 2008). Thus, identification and comparison of genomic regions governing the spikelet number and heading date will provide us useful information for genetic improvement of these two traits.

FLOWERING LOCUS T (*FT*) encoding a PEBP protein that could be transported from the leaf phloem to shoot apical meristem to initiate floral transition is a well-conserved florigen gene across flowering plants (Tsuji and Taoka, 2014). The ortholog gene of *Arabidopsis FT* in wheat is *FT-1* (also named as *Vrn-3*) (Yan *et al*., 2006). Growing evidence suggests that beyond flowering, *FT-1* also plays an important role in wheat spikelet development (Sakuma and Schnurbusch, 2020). For example, an absence of *FT-B1* was found an increase in spikelet number when grown under different temperature regimes (Dixon *et al*., 2018a; Finnegan *et al*., 2018). Brassac *et al*. (2021) identified a non-synonymous mutation in *FT-B1* that mainly influenced TSN with a minor effect on heading date. *FT-A1* with variations in the promoter or exon might influence the spikelet number and heading date (Chen *et al*., 2020b; Yu *et al*., 2017). Although some studies have identified QTL associated with spikelet number and heading date in the flanking region of *FT-D1* (Chen *et al*., 2020b; Isham *et al*., 2021), further characterization of the genetic control of *FT-D1* in spikelet number using transgenic technology is still an area to be elucidated.

In this study, we reported the mapping of stable QTL for total spikelet number (TSN) and heading date (HD) using recombinant inbred lines (RILs) derived from a cross between Hesheng2hao (HS2) and Nongda4322 (4332). Of ten genomic regions harbouring 15 stable QTL, three had pleiotropic effects for total spikelet number and heading date. One major QTL for TSN and HD on chromosome 7DS was further validated. A causal G indel in the third exon of *FT-D1* located in the fine-mapping interval was highly associated with these two traits. Furthermore, analysis of mutant lines developed by CRISPR/Cas9 provided genetic evidence for the function of *FT-D1* in regulating spikelet number and heading date.

Results

Phenotypic performance of the two parents and RIL population

Based on the phenotypic data of the two investigated traits collected from two parents in six environments, we found that 4332 had higher total spikelet number (TSN) than that of HS2 across all environments (Figure 1a,b). In addition, 4332 showed significantly delayed heading date (HD) in E4 and E5 environments when compared with HS2 (Figure 1c). Transgressive segregation was observed for each trait in the RIL population (Figure S1). TSN displayed normal distribution, whereas HD exhibited asymmetrical distribution (Figure S1). Both traits showed high broad-sense heritability (H_b^2; TSN, 0.95; HD, 0.96). Pairwise correlation analysis showed a positive correlation between TSN and HD ($r = 0.472$).

Identification of genomic regions harbouring stable QTL for spikelet number and heading date

Quantitative trait locus that could be detected in ≥3 individual environments and the combined analysis (BLUP) are regarded as 'stable QTL'. According to the criterion, 15 stable QTL for TSN and HD were identified within 10 genomic regions of nine chromosomes (1B, 2A, 3B, 3D, 5B, 5D, 6B, 7A and 7D) (Figure 2, Table S1). 'Putative QTL' that could not meet this criterion are also listed in Table S1 and shown in Figure 2.

Five stable QTL on chromosome arms 1BL, 3BL, 5DS and 7AL were found to have effects on TSN but with no significant effect on HD (Figure 2, Table S1). The QTL region on chromosome arm 1BL harboured a QTL (*QTsn.cau-1B.1*), with 4332 contributing the allele associated with increased TSN. *QTsn.cau-3B.1* was flanked by the markers *BS00037536_51* and *Excalibur_c30527_559* on the chromosome arm 3BL, with the favourable allele contributed by 4332. In addition, HS2 conferred effects for increasing TSN at the *QTsn.cau-5D.1* locus. Two adjacent TSN QTL (*QTsn.cau-7A.1* and *QTsn.cau-7A.2*) were identified on chromosome arm 7AL, with the superior alleles from 4332.

Four stable QTL regions on chromosome arms 5BL, 6BL and 7AS mainly influenced HD (Figure 2, Table S1). A stable QTL on chromosome arm 5BL was designated as *QHd.cau-5B*, with the positive allele from 4332. *QHd.cau-6B* was flanked by markers *Ex_c17379_1431* and *BS00034339_51* on 6BL, and HS2 conferred the allele for delayed HD. Two stable QTL, *QHd.cau-7A.1* and *QHd.cau-7A.2*, located in an adjacent interval on chromosome 7AS, only contributed 1.75%–6.11% and 2.91%–5.29% of the phenotypic variation, respectively, in the detected environments.

The stable QTL regions on chromosome arms 2AL, 3DS and 7DS could simultaneously influence TSN and HD (Figure 2, Table S1). A major QTL for TSN (*QTsn.cau-2A.1*) was detected on chromosome arm 2AL, which accounted for 12.50%–25.48% of the observed variation. In addition, *QHd.cau-2A* was detected in this region flanked by markers *CAP8_c607_659* and *BS00022301_51*. Two QTL (*QTsn.cau-3D* and *QHd.cau-3D*) on chromosome arm 3DS shared the uniform confidence interval, and the flanking markers were *wsnp_Ex_c2258_4232538* and *Ra_c4231_465*. A QTL controlling TSN on chromosome 7DS (*QTsn.cau-7D*) which explained 15.19%–30.93% of the phenotypic variation was identified over all environments. In addition, one major QTL for HD (*QHd.cau-7D*) was co-located with *QTsn.cau-7D*, which explained 39.13%–54.32% of the phenotypic variation. For both regions on chromosome arms 2AL and 7DS, 4332 contributed the alleles for increased TSN but delayed HD. Different from that of chromosome arms 2AL and 7DS, 4332 provided the allele that was associated with delayed heading on chromosome 3DS, whereas HS2 conferred the increasing alleles for TSN.

Fine mapping of the QTL on chromosome 7DS

To delimit the genomic interval of QTL on the short arm of chromosome 7D (*QTsn/Hd.cau-7D*), we used the linkage map of 7DS consisting of 23 markers that had been reported by Chen *et al*. (2020a) to conduct the first step of fine mapping. *QTsn/Hd.cau-7D* was further mapped to the genomic region flanked by markers *Xcau.7D-3* and *Xcau.7D-5,* and the corresponding physical interval was from 56.9 Mb to 72.5 Mb according to IWGSC (International Wheat Genome Sequencing Consortium) RefSeq v1.0 (IWGSC, 2018) (Figure 3a). Next, eight SSR markers were used to screen the segregation populations of RIL120, a residual heterozygous line that showed heterozygosity within the interval of *QTsn/Hd.cau-7D* (Chen *et al*., 2020a). Consequently, eight recombinants, designated as NF1~NF8 (NF, used for deriving NIL families), were detected that had crossover breakpoints within the *QTsn/Hd.cau-7D* region (Figure 3b). NF1~NF8 were self-pollinated to produce corresponding segregation

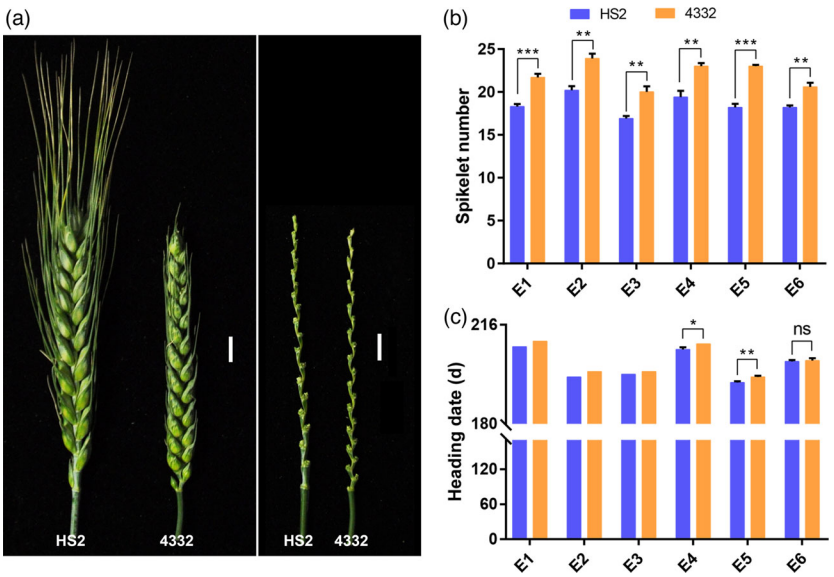

Figure 1 Spike morphologies and phenotypic data of HS2 and 4332. (a) Spikelet number (left) and rachis (right) of HS2 and 4332 grown in Beijing. The bars represent 1 cm. (b, c) Statistical analysis of heading date (b) and spikelet number (c) in HS2 and 4332. Values are means ± standard deviations (SD). Only one repeat was measured for HD at E1, E2 and E3 environments. E1, 2014–2015 Hebei; E2, 2014–2015 Shandong; E3, 2014–2015 Shanxi; E4, 2015–2016 Hebei; E5, 2015–2016 Shandong; E6, 2015–2016 Shanxi. Significant differences are indicated by * ($P < 0.05$), ** ($P < 0.01$), *** ($P < 0.001$), ns (no significant difference) (Student's *t*-test).

families, and the values for TSN and HD were compared between two homozygous groups in each NF segregation family (Figure 3b). No significant difference for TSN and HD was detected in NF4, whereas NF^{4332} (with 4332 haplotype) had 2.59%–6.25% higher TSN ($P < 0.01$) and headed later 0.7–2.4 days ($P < 0.05$) than those of NF^{HS2} (with HS2 haplotype) in NF1~3 and NF5~8 (Figure 3b). Collectively, *QTsn/Hd.cau-7D* was delimited into the interval of approximately 6 Mb flanked by the markers *Xcau.7D-4* and *Xcau.7D-7* (Figure 3b).

To further map the gene(s) associated with TSN and HD, BC_5F_2 population was developed by backcrossing RIL222 to 4332 (as the recurrent parent). Four polymorphic InDel markers (*7D-ID-6*, *7D-ID-33*, *7D-ID-8* and *7D-ID-12*) were developed and anchored to the interval between *Xcau.7D-4* and *Xcau.7D-7* according to the physical positions (Figure 3c, Tables S2 and S3). Using these new markers, BC_5F_2 plants showing heterozygosity within the interval *Xcau.7D-4~7D-ID-12* were self-pollinated to conduct the next fine-mapping step. Ultimately, nine recombinants were screened from different populations, including four from BC_5F_3 (BF3-1 to BF3-4), four from BC_5F_4 (BF5-1 to BF5-4) and one from NF3 (NF3-1) (Figure 3c). Subsequently, nine corresponding sets of NILs derived from these nine recombinants were planted in three locations (Table S4). Significant differences in TSN and HD were observed between NIL^{HS2} and NIL^{4332} derived from BF3-1~4 and BF5-1~3 across all environments ($P < 0.001$) (Figure 3c). However, there was no significant difference for TSN and HD between NIL^{HS2} and NIL^{4332} derived from BF5-4 and NF3-1 in at least two locations (Figure 3c). Based on these results, *QTsn/Hd.cau-7D* was narrowed down to 2.73 Mb physical region flanked by markers *7D-ID-6* and *7D-ID-9* (Figure 3).

To estimate the additive and dominance effects of *QTsn/Hd.cau-7D*, the TSN and HD of NF6 family were selected for further analysis, including 145 heterozygous plants and 160 homozygous plants with alternative haplotypes across the interval from *Xcau.7D-2* to *Xcau.7D-7*. Additive effects were observed for both TSN (d/a = −0.05) and HD (d/a = 0.18) (Table S5).

Cloning of the candidate gene *FT-D1*

Based on the wheat gene annotation database (IWGSC, 2018), the finely mapped genomic interval of *QTsn/Hd.cau-7D* encompassed 34 high-confidence genes, including *TraesCS7D01G111600*, a well-known *FT* gene controlling flowering (Yan *et al.*, 2006) (Table S6). To anchor the candidate genes, we firstly analysed the expression patterns of the 34 genes on the Wheat eFP Browser (http://bar.utoronto.ca/efp_wheat/cgi-bin/efpWeb.cgi; Ramirez-Gonzalez *et al.*, 2018). A total of 11 genes were found to be mainly expressed in shoot apical meristem, leaf and/or spike, which will most probably influence heading date and/or spikelet development (Table S7). Moreover, we investigated the sequence variations of these 11 genes in two parents according to the resequencing data. An indel of one G was detected between HS2 and 4332 within the third exon (+840 bp downstream of the translation start codon ATG) of *TraesCS7D01G111600* (*FT-D1*) (Figure 4a, Table S6). There was no other variation between two parents by amplifying a ~5.5 kb genomic sequence of *FT-D1* including 3.3 kb-upstream sequence, exons, introns and 1.2 kb-downstream sequence from HS2 and 4332 (Figure S2). The genotypes of HS2 and 4332 were named FT-D1(G) and FT-D1(ΔG), respectively (Figure 4a). As a consequence, the deletion of one G in 4332 which occurred outside the PEBP domain led to a frameshift mutation of amino acid sequence (Figure S3), revealing a new lipoprotein attachment site with two disulphide bonding sites (Bonnin *et al.*, 2008). Based on the polymorphism of *FT-D1* between HS2 and 4332, a semi-thermal asymmetric reverse PCR (STARP) marker (*SFT-D1*) was developed to genotype the RILs (Figure 4b). Notably, the homozygous and heterozygous genotypes can be easily identified by the *SFT-D1* marker (Figure 4c). As expected, *SFT-D1* was located to the finely mapped interval of *QTsn/Hd.cau-7D* (Table S3). Moreover, *SFT-D1* was used to genotype the seven NF families (NF1~3 and NF5~8). The result of *t*-test indicated that *FT-D1* was associated with delayed HD and increased TSN (Figure 4d).

Phenotypic analyses of homozygous and transgene-free *ft-D1* mutants in wheat

To determine whether *FT-D1* was associated with the TSN and HD in wheat, CRISPR/Cas9-mediated gene editing was performed to knock out *FT-D1* in a photoperiod insensitive cultivar 'CB037' background, in which the genotype of *FT-D1* was the same as that in HS2 (Figures S4 and S5). Sequence analysis showed that all mutations occurred in the sgRNA-2 target site (target-2) in the first exon (Figure 5a). After that, three homozygous *ft-D1* mutant

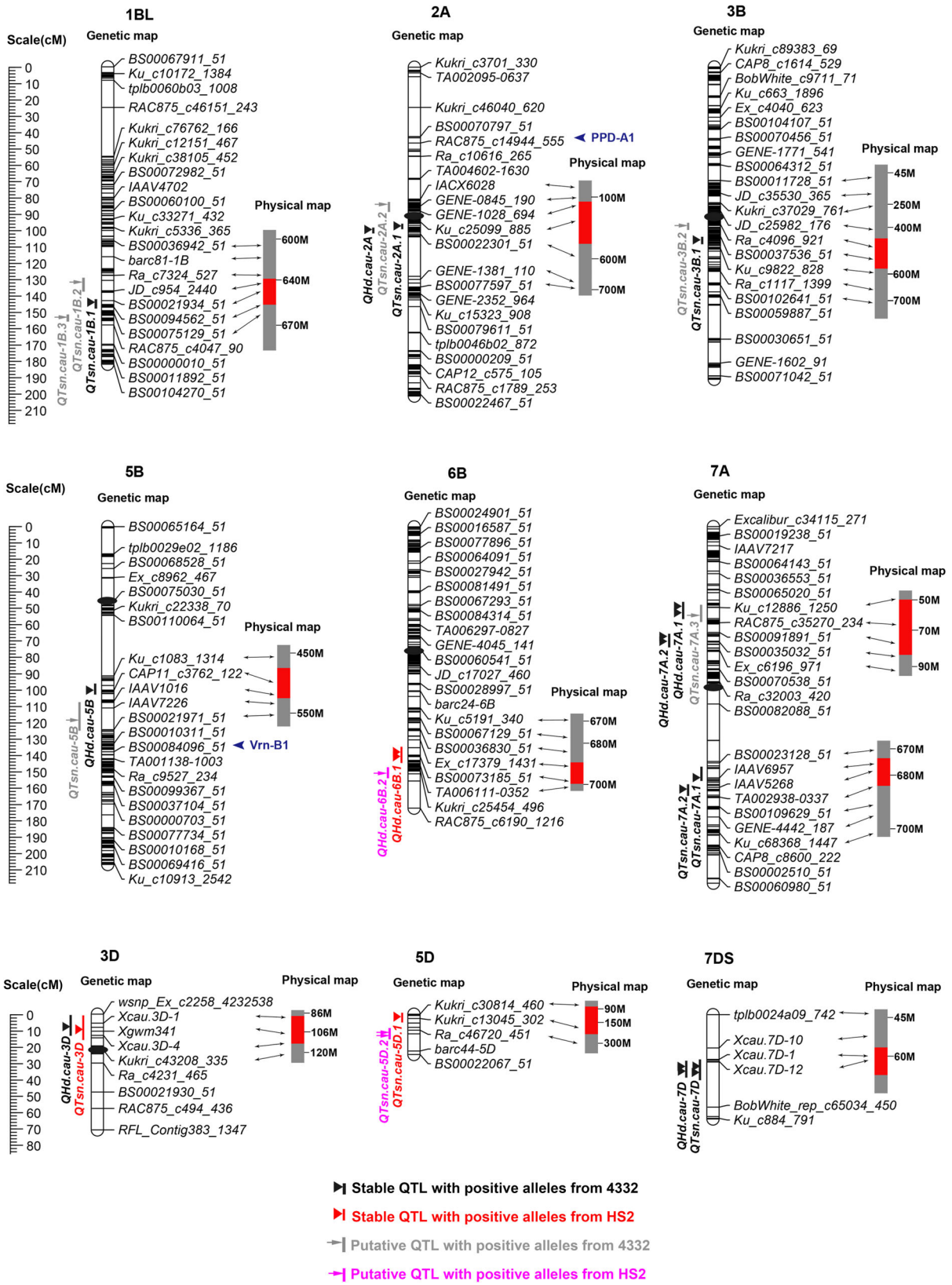

Figure 2 Chromosomal and physical locations of QTL regions associated with total spikelet number per spike (TSN) and heading date (HD). Three centimorgan (cM) scales are shown on the left. Black ellipses on chromosome bars indicate the approximate positions of the centromeres. Vertical bars represent the confidence interval for the location of each QTL. Black and red triangles indicated that positive alleles of stable QTL were contributed by 4332 and HS2, respectively. Grey and pink arrows indicate that positive alleles of putative QTL were contributed by 4332 and HS2, respectively. Red bars on the physical map represent the approximate positions of the QTL identified in the present study. The known positions of *Ppd-A1* and *Vrn-B1* are presented in blue arrows.

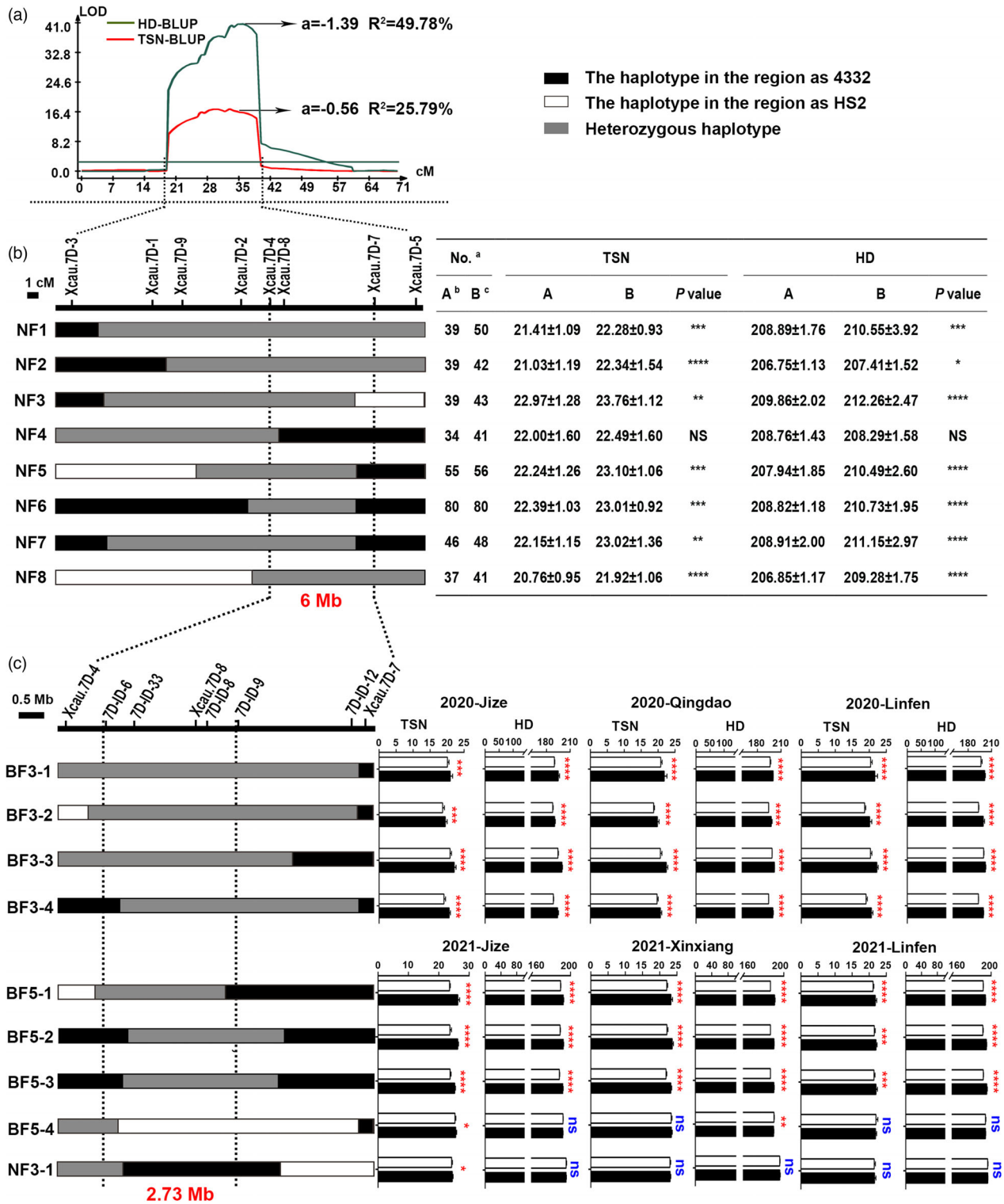

No. [a]		TSN			HD		
A [b]	B [c]	A	B	*P* value	A	B	*P* value
39	50	21.41±1.09	22.28±0.93	***	208.89±1.76	210.55±3.92	***
39	42	21.03±1.19	22.34±1.54	****	206.75±1.13	207.41±1.52	*
39	43	22.97±1.28	23.76±1.12	**	209.86±2.02	212.26±2.47	****
34	41	22.00±1.60	22.49±1.60	NS	208.76±1.43	208.29±1.58	NS
55	56	22.24±1.26	23.10±1.06	***	207.94±1.85	210.49±2.60	****
80	80	22.39±1.03	23.01±0.92	***	208.82±1.18	210.73±1.95	****
46	48	22.15±1.15	23.02±1.36	**	208.91±2.00	211.15±2.97	****
37	41	20.76±0.95	21.92±1.06	****	206.85±1.17	209.28±1.75	****

Figure 3 Fine-mapping of *QTsn/Hd.cau-7D*. (a) The results of QTL mapping using genetic linkage map with 23 markers. 'a' and 'R^{2}' represent additive effect and explained phenotypic variation rate, respectively. (b) *Left side* is the graphical genotypes of the recombinants (NF1~NF8). On the *right side*, the means of TSN and HD (mean ± SD) of the homozygous plants in NF families are presented. [a]'No.', number of plants in each NF family. [b]'A', Plants with HS2 alleles, [c]'B', Plants with 4332 alleles. (c) Further fine-mapping of *QTsn/Hd.cau-7D* using four new markers. *Left side* is the graphical genotypes of the recombinants. Right side is the comparisons of TSN and HD between NIL^{HS2} and NIL^{4332} derived from corresponding recombinants at three environments. White, grey and black rectangles represent HS2, heterozygous and 4332 alleles, respectively. Significant differences are indicated by * ($P < 0.05$), ** ($P < 0.01$), *** ($P < 0.001$), **** ($P < 0.0001$) (Student's *t*-test).

lines containing mutations only in *FT-D1* were obtained and subsequently designated as ko-1, ko-2 and ko-3 (Figure 5a, Figure S6). Specifically, ko-1 was mutated by the deletion of a guanine nucleotide (G), ko-2 was disrupted by the deletion of two G, and ko-3 carried seven nucleotide deletions in D genome (Figure 5a, Table S8). Protein sequence analysis revealed that those mutations resulted in amino acid changes and premature termination (Figure S7). Furthermore, these three lines were confirmed to be transgene-free by genomic PCR with a primer set recognizing the sequence of the CRISPR/Cas9 construct (Figure S8). Field phenotypic analysis showed that the heading date of all three mutant lines was 2–3 days later than that of CB037, and there was no significant difference between CB037 and negative control (NC) (Figure 5b,e). Further analysis revealed that the spikelet number of the three *ft-D1* mutant lines was significantly higher than that of wild type (WT, CB037) ($P < 0.01$) (Figure 5c,f). In addition, we observed that the plant height and spike length in *ft-D1* mutants were all significantly elevated compared with that of CB037 (Figure 5c,d,g,h), whereas only ko-3 showed significantly higher grain number per spike (GNS) compared with that of CB037 (Figure 5i). Taken together, these results revealed that *FT-D1* gene played an important role in the regulation of spikelet number and heading date.

Association analysis and implication in breeding of *FT-D1*

In further exploration of the evolution and domestication of *FT-D1*, the marker *SFT-D1* was used to genotype a diversity panel of wheat accessions, including 1430 common wheat (BBAADD) and 88 *Aegilops tauschii* (DD) from different countries (Tables S9–S11). All *Ae. tauschii* presented the FT-D1(G) allele, indicating that the deletion of one G in *FT-D1* might occur after the formation of allohexaploid species (Figure 4c, Table S9). To determine the distribution of the FT-D1(G) or FT-D1(ΔG) allele in relation to the origin of geographic area, a total of 1412 hexaploid wheat accessions with known origin were used for analysis (Tables S10 and S11). In China, FT-D1(G) was the prevalent allele in Yellow and Huai River Valleys Facultative Wheat Zone (92.87%) and Northern Winter Wheat Zone (86.1%) (Figure 6a, Table S10). By contrast, up to 84.0% of the common wheat accessions from foreign countries carried the FT-D1(ΔG) allele (Figure 6a, Table S11). In addition, the FT-D1(ΔG) allele occurred at a higher frequency (62.3%–67.7%) in Xinjiang Winter-Spring Wheat Zone, Southwestern Autumn-Sown Spring Wheat Zone, and Middle and Lower Yangtze Valleys Autumn-Sown Spring Wheat Zone (Figure 6a, Table S10).

To investigate the implications of our findings on wheat breeding, we analysed the effects of the FT-D1(ΔG) and FT-D1(G) allele on TSN and HD in a diversity panel of 150 accessions in three environments (Figure 6b, Table S12). As expected, the accessions with FT-D1(ΔG) allele had more TSN, but with a delayed heading date than those with the FT-D1(G) allele ($P < 0.01$) across all three environments (Figure 6b, Table S12). These results indicated that *FT-D1* was conserved in the hexaploid wheat and FT-D1(ΔG) allele was effective for TSN and HD in different genetic backgrounds.

Discussion

Pleiotropic QTL for spikelet number and heading date on chromosome arms 2AL, 3DS and 7DS

Spike morphogenesis in wheat is subdivided into spike initiation and growth phases (Sreenivasulu and Schnurbusch, 2012). Theoretically, the more spikelet number could be attributed to a longer thermal duration for spikelet primordia production and/or a faster rate of spikelet production, whereas the former was more closely associated with the increased spikelet production than the latter (Gaju *et al*., 2009; Guo *et al*., 2018a). Consistent with this, genes associated with heading date are always employed in manipulation of spikelet number in wheat. For example, photoperiod insensitive alleles of *Ppd-1* brought forward the time of terminal spikelet, and hence reduced the spikelet number and GNS (Guo *et al*., 2018b; Snape *et al*., 2001). *VRN1* and/or *FUL2* mutations delayed flowering initiation with highly significant effects on spikelet number (Li *et al*., 2019). The effect of *Eps-Am1* is to shorten the vegetative and spike initiation phases, thereby producing fewer spikelets (Lewis *et al*., 2008).

Here, we also found that heading date was significantly positively correlated with TSN ($r = 0.472$, $P < 0.01$). Moreover, three of seven stable QTL for heading date (*QHd.cau-2A*, *QHd.cau-3D* and *QHd.cau-7D*) were associated with TSN (Figure 2, Table S1), providing further genetic evidence that the heading date co-regulated with spikelet differentiation and the maximum spikelet number per spike determination (Abeledo *et al*., 2002). The superior alleles for increasing TSN and HD in the QTL regions on chromosome arms 2AL and 7DS were provided by 4332. Therefore, selection of these QTL for a higher spikelet number would be inevitably accompanied by a delay of heading date and vice versa. However, in the QTL region on chromosome 3D, HS2 carried the positive allele for increasing TSN as well as advancing HD. These results indicated that the mechanism of the QTL region on chromosome 3D controlling HD and spikelet number is different from that of the QTL regions on chromosomes 2A and 7D. Collectively, we proposed that these QTL could be attractive targets for marker-assisted selection to develop high spikelet number or early flowering varieties.

A single nucleotide deletion of *FT-D1* contributed to increased spikelet number and delayed heading date

Here, we demonstrated that a single nucleotide deletion of *FT-D1* would be the causal mutation of increased spikelet number but delayed heading date. This single nucleotide (G) deletion in the third exon of *FT-D1* was detected in 4332, which led to a frameshift mutation of amino acid sequence (Figure 4a, Figure S3). Compared with previous studies, we found that this variation was relatively conservative in different wheat materials. For example, Bonnin *et al*. (2008) analysed the nucleotide polymorphisms of the D copy *FT* in wheat and observed an insertion–deletion of one G in the third exon. The 1-bp deletion of G was also found in 2174 but not in Jagger by Chen *et al*. (2010). In molecular breeding, functional markers are very useful for enhancing the precision and accuracy in marker-assisted selection (MAS) of the target gene (Collard and Mackill, 2008). Hence, the development of markers based on the causal single nucleotide deletion of *FT-D1* can directly differentiate the alleles conferring increased spikelet number but delayed heading date. Recently, a new genotyping method named semi-thermal asymmetric reverse PCR (STARP) with advantages of high accuracy, simple assay design, low operational costs and compatibility for a variety of platforms, was developed by Long *et al*. (2017). Based on 1-bp polymorphism, the co-dominant STARP marker *SFT-D1* was developed and mapped to the interval between *Xcau.7D-8* and *7D-ID-8* on chromosome 7D (Table S3). Collectively, this simple, robust and economical STARP marker will simplify and

Figure 4 Cloning of *FT-D1* and development of STARP marker. (a) Schematic diagram of nucleotide polymorphism for *FT-D1*. The polymorphic site and relative positions are indicated on the genomic sequence of *FT-D1*. '−' and 'Δ' represent deletion. Exons are indicated by black boxes, flanking regions and introns are indicated by black solid lines. FT-D1(ΔG) and FT-D1(G) represent 4332 and HS2 alleles, respectively. (b) STARP marker was designed according to the nucleotide polymorphism of *FT-D1*. The red hexagons and blue solid rectangles indicate nucleotides (SNP) and substituted nucleotides, respectively. *SFT-D1.F1* and *SFT-D1.F2* specially amplify FT-D1(G) and FT-D1(ΔG), respectively. TGCTGACGAC in red indicates the introduced insertion in *SFT-D1.F2*. '-' means deletion. (c) PCR products of HS2, 4332, *Ae. tauschii* (DD) and hexaploid (AABBDD) wheat accessions and progenies of recombinants amplified by STARP marker. (d) Effects of *FT-D1* in populations derived from NF1~NF3 and NF5~NF8 using *SFT-D1*. The number of plants used for test was shown on the corresponding boxes. Significant differences are indicated by * ($P < 0.05$), ** ($P < 0.01$), *** ($P < 0.001$), **** ($P < 0.0001$) (Student's *t*-test).

streamline MAS for spikelet number and heading date in wheat breeding.

Diverse functions of *FT* and *FT*-like genes

FT is known as a florigen gene promoting flowering in flowering plants. In the present study, we demonstrated the function of *FT-D1* involved in spikelet number. Recent studies showed that *FT* and *FT*-like genes had diverse roles in plant development beyond flowering and spikelet number. The result of Kinoshita *et al*. (2011) defined a new cell-autonomous role of *FT* in regulating stomatal opening. Tsuji *et al*. (2015) showed that Hd3a (FT homolog) protein accumulates in axillary meristems to promote branching in rice. *AcFT1* promotes bulb formation of onion, which adds to the growing evidence that *FT* genes play a wide role in controlling development decisions (Lee *et al*., 2013). The *ft2aft5a* mutants produced significantly increased numbers of pods and seeds per plant compared with WT in soya bean (Cai *et al*., 2020). In wheat, Shaw *et al*. (2019) reported that *FT2* (the closest paralogue of *FT-1*) played an important role in spike development and fertility. A QTL cluster on 7DS harbouring *FT-D1* was identified to be associated with grain yield, fertile spikelet number per spike and thousand kernel weight (Isham *et al*., 2021). Here, we demonstrated the multiplex roles of *FT-D1* not only on TSN and HD but also on PHT and SL using the *ft-D1* mutants, which were probably associated with the function of *FT-1* in regulating gibberellic acid (GA) genes during the spike development (Pearce *et al*., 2013). Previous studies also reported that the delayed heading allele of *RFT1* (*RICE FLOWERING LOCUS T1*) in rice increased plant height (Zhu *et al*., 2017). It is not clear whether FT is transported to organs outside the shoot apex (Lee *et al*., 2013); therefore, the new molecular mechanism of *FT-D1* controlling different traits is still worth to elucidation.

The domestication and potential implication value of *FT-D1* in wheat breeding

The spikelet is the basal unit of inflorescence and is crucial for reproduction and final yield (Cai *et al*., 2014). Considering the influence of *FT-D1* on TSN and HD, the domestication and geographic distribution of *FT-D1* alleles will be of great interest for genetic improvement in wheat breeding. FT-D1(ΔG) allele was not detected in the diploid progenitors (*Ae. tauschii*, DD) of allohexaploid wheat (BBAADD), suggesting that this allele may arise during the hexaploidization event that yielded hexaploid wheat or the process of domestication (Table S9). In China, FT-D1 (G) was the prevalent allele in Yellow and Huai River Valleys Facultative Wheat Zone (92.87%) and Northern Winter Wheat Zone (86.1%), which may be partially attributed to the cropping system that entails growing three crops in 2 years (He, 2001); that is, wheat varieties with early maturity were required to ensure planting of summer crops. By contrast, up to 84.0% common wheat accessions from foreign countries carried FT-D1(ΔG) allele. We speculate that this variant is selected due to the its favoured potential and positive impact on the grain yield (Brassac *et al*., 2021). Taken together, these data indicated that the two *FT-D1* alleles have been widely used in wheat breeding programmes to enable adaption of wheat to special environmental conditions.

The rational design of yield and quality traits is a powerful strategy for meeting the challenges of future crop breeding (Zeng *et al*., 2017). Therefore, further isolation of the genes related to grain yield potential is needed to improve the wheat yield (Sakuma and Schnurbusch, 2020). Here, we used the CRISPR/Cas9 technology to explore the role of *FT-D1* on TSN and HD. Compared with WT, *ft-D1* mutants showed higher spikelet number with minor delayed heading date. Notably, significant GNS difference was observed between ko-3 and WT. GNS is largely determined by the spikelet number and fertile florets within a spikelet (Quarrie *et al*., 2006; Sreenivasulu and Schnurbusch, 2012), and thus, the unexpected sterile spikelets of ko-1 and ko-2 possibly explained the mild significant difference in GNS from WT. Even so, the average of GNS of all mutants was higher than that of WT and the negative control (NC) (Figure 5i). These results indicated that *ft-D1* might have a potential in increasing grain yield. Thus, pyramiding *ft-D1* with other genes controlling different complex traits involved in yield could be a possible approach in improving wheat yield.

Experimental procedures

Plant materials and field trials

The mapping population containing 271 RILs was bred from a cross between Hesheng2hao (HS2) and Nongda4332 (4332) (Chen *et al*., 2020a). 4332 is a common germplasm resource characterized by high spikelet number, whereas HS2 is a high-yield line with relatively fewer spikelet numbers. The RIL population and parents were planted in a randomized complete block design with three replications at three locations (Shandong, Hebei, Shanxi) during the 2014–2015 and 2015–2016 seasons, providing data for six environments (Table S4). Each line of RILs, along with the two parents, was evenly sown in two-row plots (1.5 m long and 0.3 m apart) at a sowing rate of 30 seeds per row.

In addition, a total of 150 winter wheat accessions were selected to plant in single-row plots with three replications at the following three environments: Shanxi Linfen (2014–2015 season), Hebei Shijiazhuang (2015–2016 season) and Shaanxi Sanyuan (2015–2016 season). Segregation families derived from residual heterozygous line (RIL120) were sown in rows 1.5 m long and 0.3 m apart at a sowing rate of 20 seeds per row at Hebei during the 2016–2017 growing season. NILs derived from BC_5F_3 were planted during 2019–2020 season in Hebei Jize, Shanxi Linfen and Shandong Qingdao; NILs derived from BC_5F_4 and NF3 were planted during 2020–2021 season in Hebei Jize, Shanxi Linfen and Henan Xinxiang (Table S4). The planting pattern of all NILs was same as 150 winter wheat accessions.

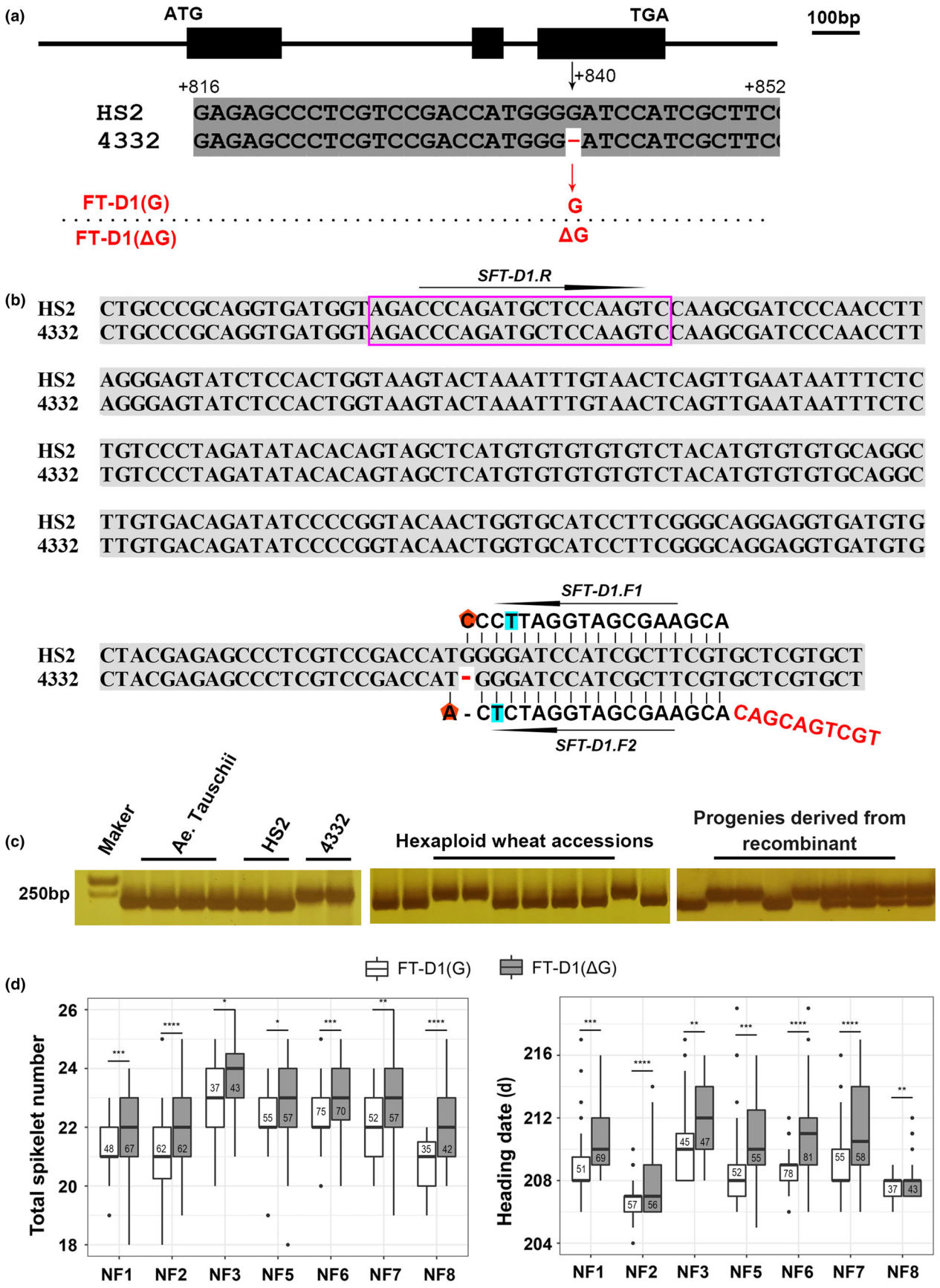
(a)
ATG
TGA
100bp
+816
+840
+852
HS2 GAGAGCCCTCGTCCGACCATGGGGATCCATCGCTTC
4332 GAGAGCCCTCGTCCGACCATGGG-ATCCATCGCTTC
FT-D1(G)
FT-D1(ΔG)
G
ΔG
(b)
SFT-D1.R
HS2 CTGCCCGCAGGTGATGGTAGACCCAGATGCTCCAAGTCCAAGCGATCCCAACCTT
4332 CTGCCCGCAGGTGATGGTAGACCCAGATGCTCCAAGTCCAAGCGATCCCAACCTT
HS2 AGGGAGTATCTCCACTGGTAAGTACTAAATTTGTAACTCAGTTGAATAATTTCTC
4332 AGGGAGTATCTCCACTGGTAAGTACTAAATTTGTAACTCAGTTGAATAATTTCTC
HS2 TGTCCCTAGATATACACAGTAGCTCATGTGTGTGTGTCTACATGTGTGTGCAGGC
4332 TGTCCCTAGATATACACAGTAGCTCATGTGTGTGTGTCTACATGTGTGTGCAGGC
HS2 TTGTGACAGATATCCCCGGTACAACTGGTGCATCCTTCGGGCAGGAGGTGATGTG
4332 TTGTGACAGATATCCCCGGTACAACTGGTGCATCCTTCGGGCAGGAGGTGATGTG
SFT-D1.F1
CCCTTAGGTAGCGAAGCA
HS2 CTACGAGAGCCCTCGTCCGACCATGGGGATCCATCGCTTCGTGCTCGTGCT
4332 CTACGAGAGCCCTCGTCCGACCAT-GGGATCCATCGCTTCGTGCTCGTGCT
A-CTCTAGGTAGCGAAGCA CAGCAGTCGT
SFT-D1.F2
(c)
Maker
Ae. Tauschii
HS2
4332
Hexaploid wheat accessions
Progenies derived from recombinant
250bp
(d)
FT-D1(G)
FT-D1(ΔG)
Total spikelet number
Heading date (d)
NF1
NF2
NF3
NF5
NF6
NF7
NF8

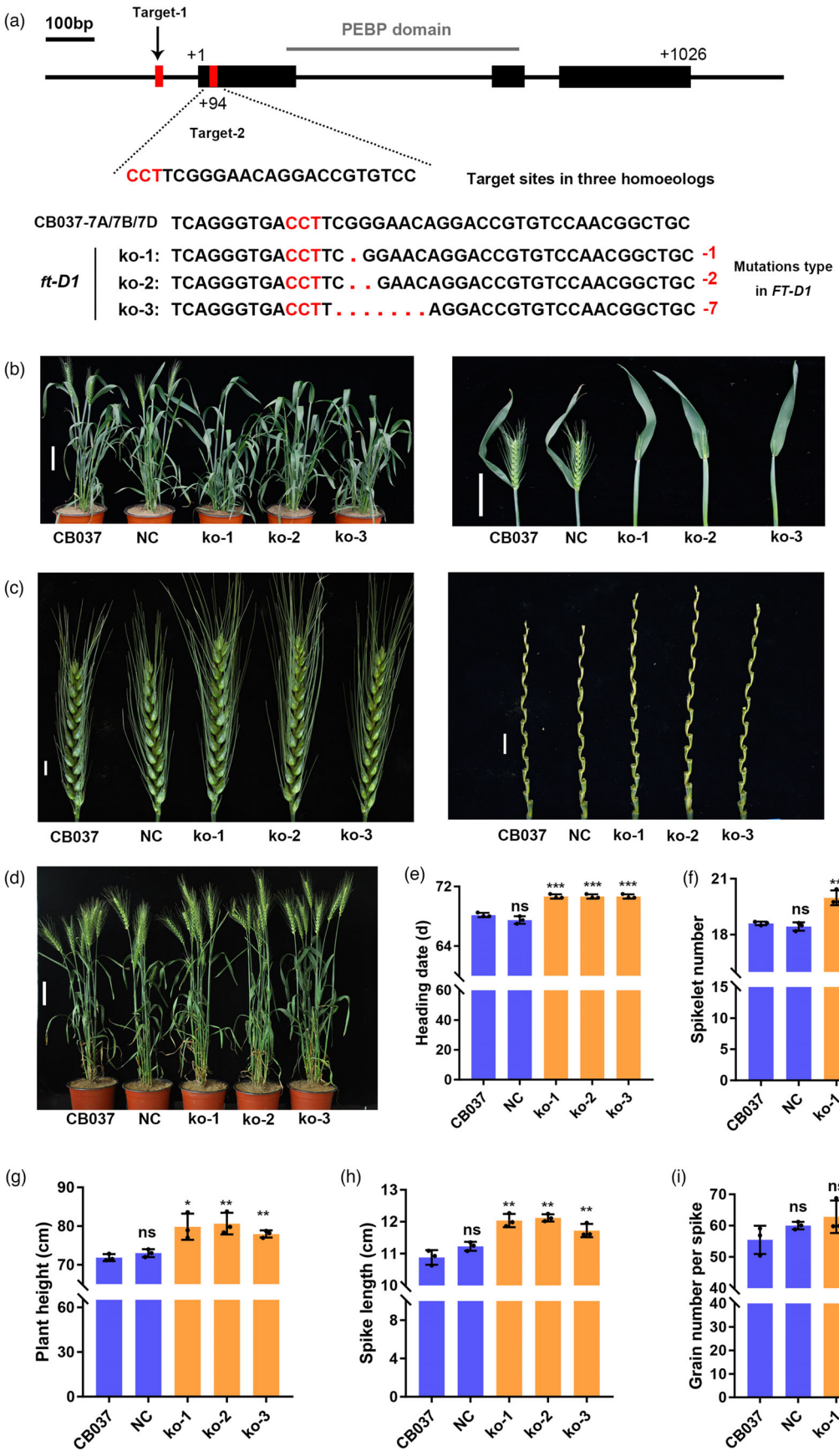

Figure 5 Phenotype of *FT-D1* knock-out mutant lines induced by CRISPR/Cas9. (a) The gene structure of *FT-1*, locations of the two target sites of *FT-D1* and mutant types of three *ft-D1* mutant lines induced by CRISPR/Cas9. Deleted nucleotides are shown by '.'. The numbers represent the number of nucleotides involved in the deletion. (b–d) Phenotypes of heading (b), spike (c) and plant height (d) of CB037, negative control (NC) and *ft-D1* mutant lines. Scale bars in (b) and (d) represent 10 cm; bars in (c) represent 1 cm. (e–i) Statistical analysis of phenotype between CB037 and *ft-D1* mutant lines. (e) heading date; (f) spikelet number; (g) plant height; (h) spike length; (i) grain number per spike. Data were means ± SD, and *t*-test was used to compare mutant lines, NC and CB037. $*P < 0.05$, $**P < 0.01$, $***P < 0.001$; $****P < 0.0001$; ns, no significant difference.

The wheat accessions, which included 1430 hexaploid wheat (967 Chinese accessions and 463 foreign accessions) (BBAADD), and 88 *Ae. tauschii* (DD) from different countries were gathered to detect the allele distribution for the target gene (Tables S9–S11).

Phenotypic evaluation in field conditions

For the RIL population, 150 winter wheat accessions and NILs, the heading date (HD) of each field plot was recorded as the developmental stage, by counting days from the sowing date to the date when approximately 50% of the spikes had fully emerged from the flag leaf sheath in each genotype. For RIL population planted at Shandong, Hebei and Shanxi during the 2014–2015, only one repeat was measured for HD. For 150 winter wheat accessions and NIL populations planted in one-row plots, the spikelet number data of each genotype were collected from five spikes of main tillers in each replicate at maturity; for RIL population planted in two-row plots, ten spikes of each genotype were measured. The resultant TSN data were the average ± SD (standard deviations) of three replicates for each environment.

For the fine-mapping families NF1~NF8, the HD of the segregation families was scored when the first head of single plant was fully visible. At maturity, the main spike of each single plant was sampled, and the TSN was assessed.

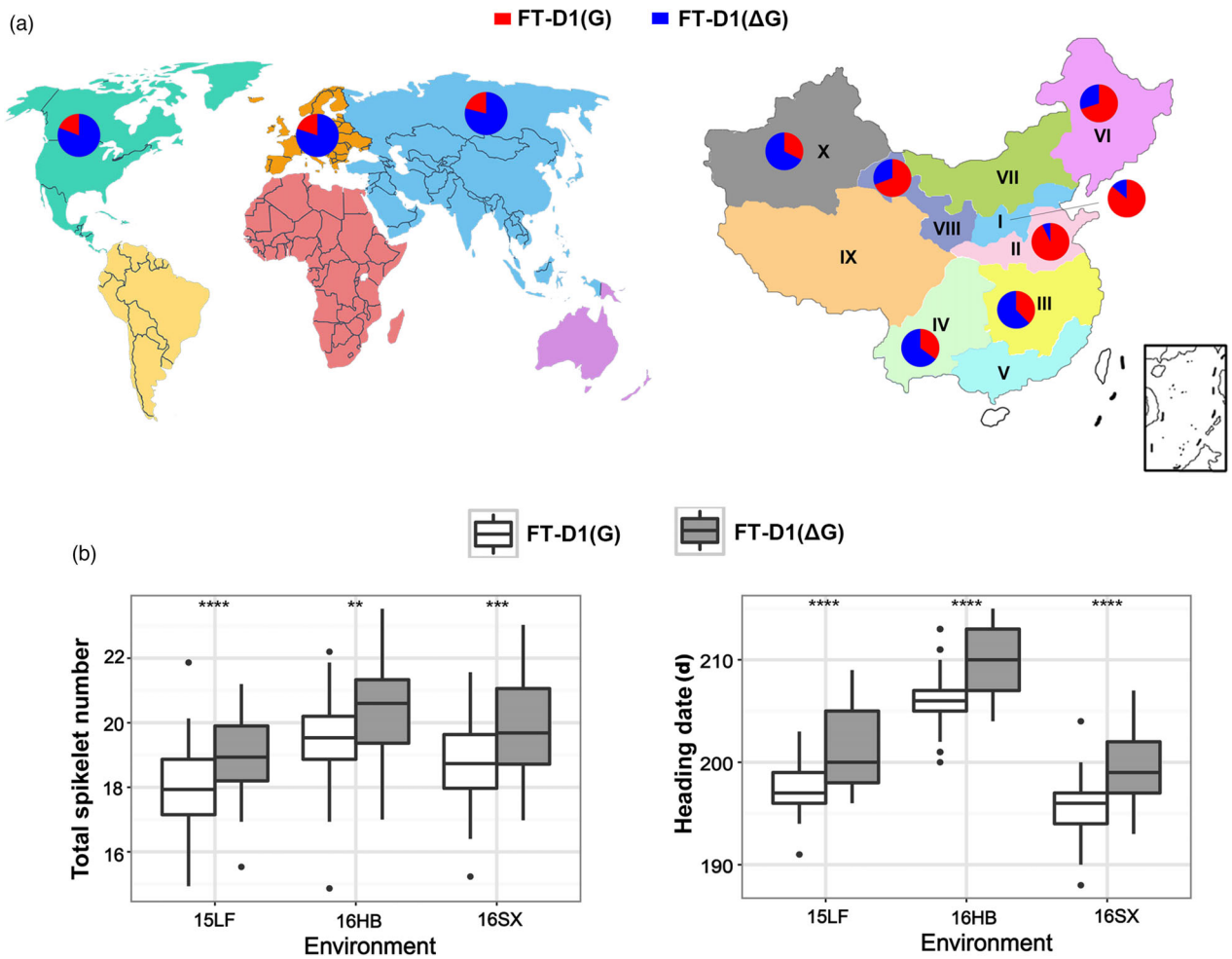

Figure 6 Geographic distributions and contributions of *FT-D1* haplotypes based on the functional STARP marker *SFT-D1*. (a) Geographic distributions of *FT-D1* haplotypes in the worldwide and Chinese accessions. I, Northern Winter Wheat Zone; II, Yellow and Huai River Valleys Facultative Wheat Zone; III, Middle and Lower Yangtze Valleys Autumn-Sown Spring Wheat Zone; IV, Southwestern Autumn-Sown Spring Wheat Zone; V, Southern Autumn-Sown Spring Wheat Zone; VI, Northeastern Spring Wheat Zone; VII, Northern Spring Wheat Zone; VIII, Northwestern Spring Wheat Zone; IX, Qinghai-Tibetan Plateau Spring-Winter Wheat Zone; X, Xinjiang Winter-Spring Wheat Zone. (b) Contributions of *FT-D1* to TSN and HD in 150 wheat accessions grown in three different environments using *SFT-D1* marker. 15LF, 2014–2015 Shanxi Linfen; 16SY, 2015–2016 Shaanxi Sanyuan; 16HB, 2015–2016 Hebei Shijiazhuang. $*P < 0.05$, $**P < 0.01$, $***P < 0.001$; $****P < 0.0001$.

Statistical analysis

The best linear unbiased prediction (BLUP) for TSN and HD across all environments was computed using SAS9.2 (SAS Institute Inc., Cary, NC) with the PROC MIXED procedure to reduce the influence of environmental effects on phenotypic variation. The descriptive statistics of RILs from each environment including the means and Pearson's correlation coefficient were analysed using software SPSS version 20.0 (SPSS, Chicago, IL). The Shapiro–Wilk test was performed with R software (V. 3.2.2; R Core Team, 2019) to test departures from normal distribution. The broad-sense heritability (H_b^2) for each trait was estimated using the lme4 package in R software (Bates *et al.*, 2015), and the formula is $H_b^2 = {}^2_g/({}^2_g + {}^2/n)$, where ${}^2_g$ is genotypic effect, σ^2 is the residual error, n is the number of environments (Xu *et al.*, 2017). Significance analysis was calculated using Student's *t*-test.

QTL analysis

The genetic linkage map of HS2/4332 RILs used in the present study had been described in Chen *et al*. (2020a). The means of each trait under six environments and the adjusted mean values of BLUP were collected for QTL analysis. QTL analysis was performed using the Windows QTL Cartographer version 2.5 software (Wang *et al*., 2012), with the composite interval mapping (CIM) method (Zeng, 1994). The parameter exploited for the QTL calculations was set according to Chen *et al*. (2020a). QTL with threshold LOD values ≥2.5 and similar confidence intervals (±2 LOD away from the peaks of likelihood ratios) were considered identical QTL and were named according to McIntosh *et al*. (2017).

InDel markers' development

The resequencing data of HS2 and 4332 had been submitted by Cheng *et al*. (2020) to the National Center for Biotechnology Information (NCBI, https://www.ncbi.nlm.nih.gov/sra) under accession number PRJNA533588. Insertion/deletions within the interval between markers *Xcau.7D-4* and *Xcau.7D-7* were searched according to the resequencing data of HS2 and 4332. Then, the corresponding sequences were blasted and used to design primers in Primer3 v.0.4.0 (http://bioinfo.ut.ee/primer3-0.4.0/). The sequences of new InDel markers are listed in Table S2. The 10 μL PCR system followed as 5 μL 2×*Taq* PCR StarMix, 2 μL primer, 2 μL 50–100 ng/μL DNA template and 1 μL H_2O.

Fine mapping of *QTsn/Hd.cau-7D*

We adopted a recombinant-derived progeny testing strategy to fine map *QTsn/Hd.cau-7D*. Briefly, we used segregation families derived from two generations after self-pollinated of RIL120, a residual heterozygous line that has been identified and used in our previous study (Chen *et al*., 2020a), to screen recombinants. Then, each recombinant was self-pollinated and the derived-homozygous lines were phenotypically evaluated to narrow down the target interval. In addition, RIL222 harboured HS2 alleles within the *QTsn/Hd.cau-7D* was backcrossed to 4332 (4332 as recurrent parent) to obtain BC_5F_2 population. Using four new markers, four, four and one recombinants were screened from BC_5F_3, BC_5F_4 and progenies of NF3, respectively. Subsequently, 10–15 lines with homozygous HS2 alleles and 10–15 lines with homozygous 4332 alleles (NILs) were randomly selected from corresponding generations of nine recombinants, which were planted in three locations to evaluate phenotype (Table S4).

For the QTL controlling TSN and HD on chromosome arm 7DS, NF6 derived from RIL120 were divided into three genotypic classes (homozygous families and heterozygous families) based on their corresponding marker genotypes. The inheritance mode of an individual QTL can be classified into four categories: additive ($d/a \leq 0.20$), partial dominance ($0.20 < d/a < 0.80$), dominance ($0.80 \leq d/a < 1.20$) and overdominance ($d/a \geq 1.20$), as described in the previous studies (Li *et al*., 2017; Zhai *et al*., 2018).

Cloning the genomic DNA of *FT-D1*

Based on the sequence alignment, three set of primers for *FT-D1* (*TraesCS7D01G111600*) were designed to amplify HS2 and 4332 (Table S2). PCR products were gel-purified and cloned into the pGEM-T Easy Vector (Promega) for sequencing. Nucleotide sequence alignments of parents were performed using DNAMAN 8 (8.0.8.789).

STARP marker development

For distinguishing an insertion–deletion of one G between HS2 and 4332, we developed semi-thermal asymmetric reverse PCR markers (STARP), as described by Long *et al*. (2017) with minor modifications. STARP marker included two asymmetrically modified AMAS primers and their same reverse primer. AMAS-primer 1 (*SFT-D1.F1*) was designed to uniquely amplify the FT-D1(G) allele. Meanwhile, the AMAS-primer 2 (*SFT-D1.F2*), with its introduced 10 bp insertion (TGCTGACGAC) at 5′ terminus, could specially amplify the FT-D1(ΔG) allele. Nucleotide substitution principle was followed as depicted in Long *et al*. (2017). Two AMAS primers and their reverse primer were mixed in a proportion of 1:1:2 and diluted. The PCR program was 95 °C for 5 min, followed by 9 cycles of 3-step touchdown PCR program: 95 °C for 30 s, 68 °C for 30s and 72 °C for 30 s, with the annealing temperature being decreased by 1 °C per cycle and then 30 cycles of the 3-step PCR program as usual. To increase resolution, a 10% non-denatured polyacrylamide gel electrophoresis (PAGE) was adopted to separate the length polymorphism.

Construction of CRISPR/Cas9 transgenic vector

Two target sites were designed to recognize regions in the promoter sequence and coding sequence of *FT-1* on the website E-CRISP Design (http://www.e-crisp.org/E-CRISP/), respectively (Table S2). We blasted these two target sequences on the Ensembl Plants database (Howe *et al*., 2019; http://plants.ensembl.org/index.html) and found that the target-1 matched *FT-D1* perfectly but mismatched with *FT-A1* and *FT-B1*, whereas target-2 targeted three homoeologous genes of *FT-1* (Table S2). Fragments were amplified from the pCBC-MT_1T_2 plasmid using four primers containing two target sites of sgRNA with two *Bsa*I restriction site. The PCR products were digested with *Bsa*I and inserted into *Bsa*I-digested pBUE414 to yield the fused expression vector. The resulting CRISPR/Cas9 construct was bombarded into the cultured immature embryo of CB037, a spring, photoperiod insensitive (carried a 2089 bp deletion in *Ppd-D1* promoter) wheat cultivar with high transformability (Figure S4) (Beales *et al*., 2007; Wang *et al*., 2017).

Homozygous mutant line development and phenotypic evaluation

T_0 mutants were identified via amplifying the genomic DNA using a set of conserved primer, which were planted in a greenhouse under LD photoperiod and controlled temperature (24 °C during 16-h light period and 20 °C during 8-h dark period). Because target-2 could target three homoeologous genes of *FT-1*, primer pairs *c2-A1*, *c2-B1* and *c2-D1* specific for *FT-A1*, *FT-B1* and *FT-D1*,

respectively, were developed to analyse the mutant type of each transgenic plants. For T_0 and T_1 generations, the PCR products of each transgenic plant were cloned into pEASY-T1 simple cloning vector (TransGen Biotech, Beijing, China), and the number of randomly sequenced clones was at least 30 (T_0) and 6 (T_1). The PCR products of T_2 and T_3 generations were sequenced directly. In addition, a marker (CR-VT) was designed for detecting CRISPR/Cas9 (Table S2). Homozygous and transgene-free lines (*ft-D1*) were obtained by self-pollinating of T_0 twice. The detailed information for the mutant genotypes of *ft-1* in T_0 to T_3 generations is listed in Table S8. CB037 (WT), *ft-D1* (T_4) and negative control (NC) were planted in the field of Beijing. A randomized complete block experiment with three replications was set, each replication of each material contained two rows. Before harvest, we measured plant height from eight plants in each row. Similarly, the data of spike length and spikelet number were collected from eight main spikes in each row. Ultimately, the mean of the heading date, plant height, spike length and spikelet numbers were collected from three replications. Grain number per spike was calculated by counting that of ten spikes divided by 10 after harvest.

Acknowledgements

This work was financially supported by the National Natural Science Foundation of China (91935304, 32172069 and 31991210) and Hainan Yazhou Bay Seed Laboratory (B21HJ0111). The authors thank Xingguo Ye (Chinese Academy of Agricultural Sciences) for providing the seeds of CB037 and Na Song (China Agricultural University) for help with wheat transformation.

Conflict of interest

The authors declare no conflict of interests.

Author contributions

ZN conceived the project; XC developed the RIL population; ZC, LC, XC and DD performed field trail of RILs and QTL analysis; ZC, WK, FH, HX and YZ participated in fine-mapping and transgenic experiment; ZC, XC, LC and XW collected data for 150 wheat accessions used to analyse the contribution of *FT-D1*; QS, XC, JX, MX, WG, ZH, ZS, JL, HP and YY assisted in revising the manuscript; ZC and WK analysed experimental results; ZC and ZN wrote the manuscript.

References

Abeledo, L.G., Calderini, D.F. and Slafer, G.A. (2002) Physiological changes associated with genetic improvement of grain yield in barley. In *Barley Science: Recent Advances from Molecular Biology to Agronomy of Yield and Quality* (Slafer, G.A., Molina Cano, J.L., Savin, R., Araus, J.L. and Romagosa, I., eds), pp. 361–385. New York: Food Products Press.

Bates, D., Maechler, M., Bolker, B., and Walker, S. (2015) Fitting linear mixed-effects models using lme4. *J. Stat. Softw.* **67**, 1–48.

Beales, J., Turner, A., Griffiths, S., Snape, J.W. and Laurie, D.A. (2007) A pseudo-response regulator is misexpressed in the photoperiod insensitive *Ppd-D1a* mutant of wheat (*Triticum aestivum* L.). *Theor. Appl. Genet.* **115**, 721–733.

Boden, S.A., Cavanagh, C., Cullis, B.R., Ramm, K., Greenwood, J., Jean Finnegan, E., Trevaskis, B. *et al*. (2015) *Ppd-1* is a key regulator of inflorescence architecture and paired spikelet development in wheat. *Nat. Plants*, **1**, 14016.

Bonnin, I., Rousset, M., Madur, D., Sourdille, P., Dupuits, C., Brunel, D. and Goldringer, I. (2008) *FT* genome A and D polymorphisms are associated with the variation of earliness components in hexaploid wheat. *Theor. Appl. Genet.* **116**, 383–394.

Brassac, J., Muqaddasi, Q.H., Plieske, J., Ganal, M.W. and Roder, M.S. (2021) Linkage mapping identifies a non-synonymous mutation in *FLOWERING LOCUS T* (*FT-B1*) increasing spikelet number per spike. *Sci. Rep.* **11**, 1585.

Cai, Q., Yuan, Z., Chen, M., Yin, C., Luo, Z., Zhao, X., Liang, W. *et al*. (2014) Jasmonic acid regulates spikelet development in rice. *Nat. Commun.* **5**, 3476.

Cai, Y., Wang, L., Chen, L., Wu, T., Liu, L., Sun, S., Wu, C. *et al*. (2020) Mutagenesis of *GmFT2a* and *GmFT5a* mediated by CRISPR/Cas9 contributes for expanding the regional adaptability of soybean. *Plant Biotechnol. J.* **18**, 298–309.

Chen, Y.H., Carver, B.F., Wang, S.W., Cao, S.H. and Yan, L.L. (2010) Genetic regulation of developmental phases in winter wheat. *Mol. Breeding*, **26**, 573–582.

Chen, Z., Cheng, X., Chai, L., Wang, Z., Bian, R., Li, J., Zhao, A. *et al*. (2020a) Dissection of genetic factors underlying grain size and fine mapping of *QTgw.cau-7D* in common wheat (*Triticum aestivum* L.). *Theor. Appl. Genet.* **133**, 149–162.

Chen, Z., Cheng, X., Chai, L., Wang, Z., Du, D., Wang, Z., Bian, R. *et al*. (2020b) Pleiotropic QTL influencing spikelet number and heading date in common wheat (*Triticum aestivum* L.). *Theor. Appl. Genet.* **133**, 1825–1838.

Cheng, X., Xin, M., Xu, R., Chen, Z., Cai, W., Chai, L., Xu, H. *et al*. (2020) A single amino acid substitution in STKc_GSK3 kinase conferring semispherical grains and its implications for the origin of *Triticum sphaerococcum*. *Plant Cell*, **32**, 923–934.

Chouard, P. (1960) Vernalization and its relations to dormancy. *Annu. Rev. Plant Phys.* **11**, 191–238.

Collard, B.C. and Mackill, D.J. (2008) Marker-assisted selection: an approach for precision plant breeding in the twenty-first century. *Philos. Trans. R Soc. Lond. B Biol. Sci.* **363**, 557–572.

Cui, F., Ding, A.M., Li, J., Zhao, C.H., Wang, L., Wang, X.Q., Qi, X.L. *et al*. (2012) QTL detection of seven spike-related traits and their genetic correlations in wheat using two related RIL populations. *Euphytica*, **186**, 177–192.

Deng, S., Wu, X., Wu, Y., Zhou, R., Wang, H., Jia, J. and Liu, S. (2011) Characterization and precise mapping of a QTL increasing spike number with pleiotropic effects in wheat. *Theor. Appl. Genet.* **122**, 281–289.

Dixon, L.E., Farre, A., Finnegan, E.J., Orford, S., Griffiths, S. and Boden, S.A. (2018a) Developmental responses of bread wheat to changes in ambient temperature following deletion of a locus that includes *FLOWERING LOCUS T1*. *Plant Cell Environ.* **41**, 1715–1725.

Dixon, L.E., Greenwood, J.R., Bencivenga, S., Zhang, P., Cockram, J., Mellers, G., Ramm, K. *et al*. (2018b) *TEOSINTE BRANCHED1* regulates inflorescence architecture and development in bread wheat (*Triticum aestivum*). *Plant Cell*, **30**, 563–581.

Du, D., Zhang, D., Yuan, J., Feng, M., Li, Z., Wang, Z., Zhang, Z. *et al*. (2021) *FRIZZY PANICLE* defines a regulatory hub for simultaneously controlling spikelet formation and awn elongation in bread wheat. *New Phytol.* **231**, 814–833.

Finnegan, E.J., Ford, B., Wallace, X., Pettolino, F., Griffin, P.T., Schmitz, R.J., Zhang, P. *et al*. (2018) Zebularine treatment is associated with deletion of *FT-B1* leading to an increase in spikelet number in bread wheat. *Plant Cell Environ.* **41**, 1346–1360.

Fu, D., Szűcs, P., Yan, L., Helguera, M., Skinner, J.S., Zitzewitz, J., Hayes, P.M. *et al*. (2005) Large deletions within the first intron in *VRN-1* are associated with spring growth habit in barley and wheat. *Mol. Genet. Genom.* **274**, 442–443.

Gaju, O., Reynolds, M.P., Sparkes, D.L. and Foulkes, M.J. (2009) Relationships between large-spike phenotype, grain Number, and yield potential in spring wheat. *Crop Sci.* **49**, 961–973.

Gauley, A. and Boden, S.A. (2021) Stepwise increases in *FT1* expression regulate seasonal progression of flowering in wheat (*Triticum aestivum*). *New Phytol.* **229**, 1163–1176.

Gawroński, P., Ariyadasa, R., Himmelbach, A., Poursarebani, N., Kilian, B., Stein, N., Steuernagel, B. *et al*. (2014) A distorted circadian clock causes early

flowering and temperature-dependent variation in spike development in the *Eps-3A*^{m} mutant of einkorn wheat. *Genetics*, **196**, 1253–1261.

Gomez, D., Vanzetti, L., Helguera, M., Lombardo, L., Fraschina, J. and Miralles, D.J. (2014) Effect of *Vrn-1*, *Ppd-1* genes and earliness *per se* on heading time in Argentinean bread wheat cultivars. *Field Crop. Res.* **158**, 73–81.

Guo, Z., Chen, D., Roder, M.S., Ganal, M.W. and Schnurbusch, T. (2018a) Genetic dissection of pre-anthesis sub-phase durations during the reproductive spike development of wheat. *Plant J.* **95**, 909–918.

Guo, Z., Liu, G., Roder, M.S., Reif, J.C., Ganal, M.W. and Schnurbusch, T. (2018b) Genome-wide association analyses of plant growth traits during the stem elongation phase in wheat. *Plant Biotechnol. J.*, **16**, 2042–2052.

He, Z. (2001) *A history of wheat breeding in China*. Mexico: Cimmyt.

Howe, K.L., Contreras-Moreira, B., De Silva, N., Maslen, G., Akanni, W., Allen, J., Alvarez-Jarreta, J. *et al*. (2019) Ensembl Genomes 2020—enabling non-vertebrate genomic research. *Nucleic Acids Res.* **48**, D689–D695.

Isham, K., Wang, R., Zhao, W., Wheeler, J., Klassen, N., Akhunov, E. and Chen, J. (2021) QTL mapping for grain yield and three yield components in a population derived from two high-yielding spring wheat cultivars. *Theor. Appl. Genet.* **134**, 2079–2095.

IWGSC. (2018) Shifting the limits in wheat research and breeding using a fully annotated reference genome. *Science*, **361**, eaar7191.

Kinoshita, T., Ono, N., Hayashi, Y., Morimoto, S., Nakamura, S., Soda, M., Kato, Y. *et al*. (2011) *FLOWERING LOCUS T* regulates stomatal opening. *Curr. Boil.* **21**, 1232–1238.

Kippes, N., Debernardi, J.M., Vasquez-Gross, H.A., Akpinar, B.A., Budak, H., Kato, K., Chao, S. *et al*. (2015) Identification of the *VERNALIZATION 4* gene reveals the origin of spring growth habit in ancient wheats from South Asia. *Proc. Natl. Acad. Sci. USA*, **112**, E5401–E5410.

Lee, R., Baldwin, S., Kenel, F., McCallum, J. and Macknight, R. (2013) *FLOWERING LOCUS T* genes control onion bulb formation and flowering. *Nat. Commun.* **4**, 2884.

Lewis, S., Faricelli, M.E., Appendino, M.L., Valarik, M. and Dubcovsky, J. (2008) The chromosome region including the earliness *per se* locus *Eps-A*^{m} 1 affects the duration of early developmental phases and spikelet number in diploid wheat. *J. Exp. Bot.* **59**, 3595–3607.

Li, C., Lin, H., Chen, A., Lau, M., Jernstedt, J. and Dubcovsky, J. (2019) Wheat *VRN1*, *FUL2* and *FUL3* play critical and redundant roles in spikelet development and spike determinacy. *Development*, **146**, dev175398.

Li, H., Yang, Q., Gao, L., Zhang, M., Ni, Z. and Zhang, Y. (2017) Identification of heterosis-associated stable QTLs for ear-weight-related traits in an elite maize hybrid Zhengdan 958 by design III. *Front. Plant Sci.* **8**, 561.

Long, Y.M., Chao, W.S., Ma, G.J., Xu, S.S. and Qi, L.L. (2017) An innovative SNP genotyping method adapting to multiple platforms and throughputs. *Theor. Appl. Genet.* **130**, 597–607.

Ma, J., Ding, P., Liu, J., Li, T., Zou, Y., Habib, A., Mu, Y. *et al*. (2019) Identification and validation of a major and stably expressed QTL for spikelet number per spike in bread wheat. *Theor. Appl. Genet.* **132**, 3155–3167.

Ma, Z., Zhao, D., Zhang, C., Zhang, Z., Xue, S., Lin, F., Kong, Z. *et al*. (2007) Molecular genetic analysis of five spike-related traits in wheat using RIL and immortalized F_2 populations. *Mol. Genet. Genom.* **277**, 31–42.

McIntosh, R.A., Dubcovsky, J., Rogers, W.J., Morris, C. and Xia, X.C. (2017) Catalogue of gene symbols for wheat: 2017 supplement.

Muqaddasi, Q.H., Brassac, J., Koppolu, R., Plieske, J., Ganal, M.W. and Roder, M.S. (2019) *TaAPO-A1*, an ortholog of rice *ABERRANT PANICLE ORGANIZATION 1*, is associated with total spikelet number per spike in elite European hexaploid winter wheat (*Triticum aestivum* L.) varieties. *Sci. Rep.* **9**, 659813.

Pearce, S., Vanzetti, L.S. and Dubcovsky, J. (2013) Exogenous gibberellins induce wheat spike development under short days only in the presence of *VERNALIZATION1*. *Plant Physiol.* **163**, 1433–1445.

Quarrie, S., Pekic Quarrie, S., Radosevic, R., Rancic, D., Kaminska, A., Barnes, J.D., Leverington, M. *et al*. (2006) Dissecting a wheat QTL for yield present in a range of environments: from the QTL to candidate genes. *J. Exp. Bot.* **57**, 2627–2637.

Ramirez-Gonzalez, R.H., Borrill, P., Lang, D., Harrington, S.A., Brinton, J., Venturini, L., Davey, M. *et al*. (2018) The transcriptional landscape of polyploid wheat. *Science*, **361**, 662.

R Core Team. (2019) *R: A Language and Environment for Statistical Computing*. Vienna: R Foundation for Statistical Computing. http://www.r-project.org/index.html

Sakuma, S., Golan, G., Guo, Z., Ogawa, T., Tagiri, A., Sugimoto, K., Bernhardt, N. *et al*. (2019) Unleashing floret fertility in wheat through the mutation of a homeobox gene. *Proc. Natl. Acad. Sci. USA*, **116**, 5182–5187.

Sakuma, S. and Schnurbusch, T. (2020) Of floral fortune: tinkering with the grain yield potential of cereal crops. *New Phytol.* **225**, 1873–1882.

Shaw, L.M., Lyu, B., Turner, R., Li, C., Chen, F., Han, X., Fu, D. *et al*. (2019) *FLOWERING LOCUS T2* regulates spike development and fertility in temperate cereals. *J. Exp. Bot.* **70**, 193–204.

Shimada, S., Ogawa, T., Kitagawa, S., Suzuki, T., Ikari, C., Shitsukawa, N., Abe, T. *et al*. (2009) A genetic network of flowering-time genes in wheat leaves, in which an *APETALA1/FRUITFULL*-like gene, *VRN1*, is upstream of *FLOWERING LOCUS T*. *Plant J.* **58**, 668–681.

Simmonds, J., Scott, P., Leverington-Waite, M., Turner, A.S., Brinton, J., Korzun, V., Snape, J. *et al*. (2014) Identification and independent validation of a stable yield and thousand grain weight QTL on chromosome 6A of hexaploid wheat (*Triticum aestivum* L.). *BMC Plant Biol.* **14**, 191.

Snape, J., Butterworth, K., Whitechurch, E. and Worland, A. (2001) Waiting for fine times: genetics of flowering time in wheat. In *Wheat in a Global Environment* (Bedö, Z. and Láng, L., eds), pp. 67–74. Berlin: Springer.

Sreenivasulu, N. and Schnurbusch, T. (2012) A genetic playground for enhancing grain number in cereals. *Trends Plant Sci.* **17**, 91–101.

Tsuji, H., Tachibana, C., Tamaki, S., Taoka, K., Kyozuka, J. and Shimamoto, K. (2015) *Hd3a* promotes lateral branching in rice. *Plant J.* **82**, 256–266.

Tsuji, H. and Taoka, K.-I. (2014) Chapter Five - florigen signaling. In *The Enzymes* (Machida, Y., Lin, C. and Tamanoi, F., eds), pp. 113–144. Cambridge: Academic Press.

Wang, K., Liu, H., Du, L. and Ye, X. (2017) Generation of marker-free transgenic hexaploid wheat via an Agrobacterium-mediated co-transformation strategy in commercial Chinese wheat varieties. *Plant Biotechnol. J.* **15**, 614–623.

Wang, S., Basten, C. and Zeng, Z. (2012) Windows QTL Cartographer 2.5. Department of Statistics, North Carolina State University, Raleigh, NC, 2010.

Worland, A.J. (1996) The influence of flowering time genes on environmental adaptability in European wheats. *Euphytica*, **89**, 49–57.

Xu, G., Wang, X., Huang, C., Xu, D., Li, D., Tian, J., Chen, Q. *et al*. (2017) Complex genetic architecture underlies maize tassel domestication. *New Phytol.* **214**, 852–864.

Yan, L., Fu, D., Li, C., Blechl, A., Tranquilli, G., Bonafede, M., Sanchez, A. *et al*. (2006) The wheat and barley vernalization gene *VRN3* is an orthologue of *FT*. *Proc. Natl. Acad. Sci. USA*, **103**, 19581–19586.

Yan, L., Loukoianov, A., Tranquilli, G., Helguera, M., Fahima, T. and Dubcovsky, J. (2003) Positional cloning of the wheat vernalization gene *VRN1*. *Proc. Natl. Acad. Sci. USA*, **100**, 6263–6268.

Yan, L., Loukoianov, A., Blechl, A., Tranquilli, G., Ramakrishna, W., SanMiguel, P., Bennetzen, J.L. *et al*. (2004) The wheat *VRN2* gene is a flowering repressor down-regulated by vernalization. *Science*, **303**, 1640–1644.

Yao, H., Xie, Q., Xue, S., Luo, J., Lu, J., Kong, Z., Wang, Y. *et al*. (2019) *HL2* on chromosome 7D of wheat (*Triticum aestivum* L.) regulates both head length and spikelet number. *Theor. Appl. Genet.* **132**, 1789–1797.

Yasuda, S. and Shimoyama, H. (1965) Analysis of internal factors influencing the heading time of wheat varieties. *Ber. Ohara Inst. Landw. Biol. Okayama Univ.* **13**, 23–38.

Yu, K., Liu, D., Wu, W., Yang, W., Sun, J., Li, X., Zhan, K. *et al*. (2017) Development of an integrated linkage map of einkorn wheat and its application for QTL mapping and genome sequence anchoring. *Theor. Appl. Genet.* **130**, 53–70.

Zeng, D., Tian, Z., Rao, Y., Dong, G., Yang, Y., Huang, L., Leng, Y. *et al*. (2017) Rational design of high-yield and superior-quality rice. *Nat. Plants*, **3**, 17031.

Zeng, Z.B. (1994) Precision mapping of quantitative trait loci. *Genetics*, **136**, 1457–1468.

Zhai, H., Feng, Z., Li, J., Liu, X., Xiao, S., Ni, Z. and Sun, Q. (2016) QTL analysis of spike morphological traits and plant height in winter wheat (*Triticum aestivum* L.) using a high-density SNP and SSR-based linkage map. *Front. Plant Sci.* **7**, 1617.

Zhai, H., Feng, Z., Du, X., Song, Y., Liu, X., Qi, Z., Song, L. *et al*. (2018) A novel allele of *TaGW2-A1* is located in a finely mapped QTL that increases grain weight but decreases grain number in wheat (*Triticum aestivum* L.). *Theor. Appl. Genet.* **131**, 539–553.

Zhang, B., Liu, X., Xu, W., Chang, J., Li, A., Mao, X., Zhang, X. *et al*. (2015) Novel function of a putative *MOC1* ortholog associated with spikelet number per spike in common wheat. *Sci. Rep.* **5**, 12211.

Zhang, X., Liu, G., Zhang, L., Xia, C., Zhao, T., Jia, J., Liu, X. *et al*. (2018) Fine mapping of a novel heading date gene, *TaHdm605*, in hexaploid wheat. *Front. Plant Sci.* **9**, 1059.

Zhou, Y., Conway, B., Miller, D., Marshall, D., Cooper, A., Murphy, P., Chao, S. *et al*. (2017) Quantitative trait loci mapping for spike characteristics in hexaploid wheat. *Plant Genome*, **10**, 1–15.

Zhu, Y.J., Fan, Y.Y., Wang, K., Huang, D.R., Liu, W.Z., Ying, J.Z. and Zhuang, J.Y. (2017) Rice *Flowering Locus T1* plays an important role in heading date influencing yield traits in rice. *Sci. Rep.* **7**, 4918.

Supporting information

Additional supporting information may be found online in the Supporting Information section at the end of the article.

Figure S1. Histograms of the HS2/4332 recombinant inbred population for total spikelet number (TSN) and heading date (HD) based on the adjusted mean values (BLUP) collected from all environments.
Figure S2. Comparation analysis of *FT-D1* sequence between HS2 and 4332.
Figure S3. *FT-D1* peptide alignment between HS2 and 4332.
Figure S4. Comparation analysis of *Ppd-D1* promoter between Chinese Spring (CS) and CB037.
Figure S5. The gene sequence of *FT-D1* in CB037.
Figure S6. Comparison of whole gene sequences of *FT-A1* and *FT-B1* among CS (Chinese Spring), CB037 and three *ft-D1* mutants.
Figure S7. Peptides alignment between CB037 (7D) and *ft-D1* mutant lines.
Figure S8. Three transgene-free lines were identified by used a pair of primer recognizing the sequence of the CRISPR/Cas9 construct.

Table S1. Effects of stable and putative QTL for TSN and HD in individual environments.
Table S2. Sequence of primers used in this study.
Table S3. Physical location of markers on the linkage map of 7DS.
Table S4. Planting environments and planting date of materials.
Table S5. Estimation of the additive and dominance effects of *QTsn/Hd.cau-7D* on TSN and HD using NF6.
Table S6. Putative genes harbored in the interval between markers *7D-ID-6* and *7D-ID-9*.
Table S7. Expression of 11 high confidence genes according to the gene expression atlas on the Wheat eFP Browser.
Table S8. The genotypes of *ft-1* mutant lines in T_0 to T_3 generations.
Table S9. *FT-D1* genotype in 88 *Ae. Tauschii*.
Table S10. Origins and genotypes of *FT-D1* in Chinese wheat accessions.
Table S11. *FT-D1* genotype in foreign wheat accessions.
Table S12. Genotype and phenotype of 150 wheat accessions used to analyze the contribution of *FT-D1*.

